The Influence of Higher Order Modes upon the Accuracy of Dielectric Constant Determinations Using Transmission Measurement Cells for Electrolyte Solutions Having Strongly Depressed Dielectric Constants in the Gigahertz Range

* J. Krüger, E. Schollmeyer, and J. Barthel
Department of Chemistry, Regensburg University

(Z. Naturforsch. **30 a,** 1476—1480 [1975] ; received May 5, 195)

The results of absorption measurements on aqueous electrolyte solutions (KF, KI and CsF) with high dielectric loss at five frequencies (8.25; 10.015; 11.88; 27.2 and 38.5 GHz) are reported. With the help of statistical data analysis methods the influence of the higher order modes on the accuracy of the data has been investigated. The use of measuring cells whose construction is based upon the theory of time independent, sourcefree ports, in connection with a highly precise amplitude receiver, allows the analysis of attenuation produced by these solutions. Interpretation of the data obtained using transmission techniques shows that the accuracy of such attenuation measurements is limited to 0.1% by higher order modes.

1. Introduction

This paper deals with experimentation upon the limits of accuracy in the measurement of attenuation constants of electrolyte solutions in the X- and K_A-bands (using standard rectangular waveguides in the frequency ranges of $8-12.4$ GHz and $26.5-40$ GHz [1, 2]). The measurements were made according to a transmission method. The pertinent data were collected using measurement cells for the X-band [3] and the K_A-band [1, 2], which differ markedly from one another in their mechanical discontinuities, thus offering different conditions for the excitation of higher order modes. These latter can be extended up to at least the TE_{12}-mode [4, 5] within the measurement cell, since for the real values of the complex, frequency-dependent dielectric constants $\varepsilon^*(\omega) = \varepsilon' - j\,\varepsilon''$, it follows for our solutions that $\varepsilon' \geqq 14$ **. In every case, along with the excitation and propagation of higher order modes in the measurement cell, appropriate correction factors for the instrumentation must be calculated.

2. Apparatus

The main units of the measurement equipment for both frequency bands (Fig. 1) are the cw-microwave transmitter with a high frequency stability ($\Delta f / f < 10^{-4}$), the precision amplitude receiver, the mixerdiodes and the linear-logarithmic converter [1, 2, 8]. The amplitude receiver utilizes a "Phase Lock System". Transmitter and receiver are isolated from the measurement cell with isolators. All data were collected at a measurement cell temperature of

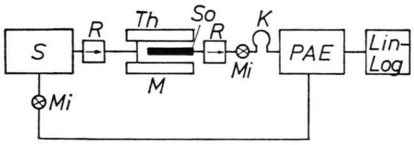

Fig. 1. Construction of the instrumentation: S — oscillator, Mi — mixerdiodes, R — isolator, M — measurement cell with thermostic housing, So — probe, K — coaxial cable, PAE — precision amplitude receiver, Lin-Log — linear logarithmic converter.

Reprint requests to Dr. J. Krüger, Fachbereich 11.2 — Experimentalphysik der Universität des Saarlandes, *D-6600 Saarbrücken.*

Present Addresses
* J. Krüger, Fachrichtung 11.2, Experimentalphysik, Universität des Saarlandes,
E. Schollmeyer, Institut für Chemiefasern, Stuttgart,
J. Barthel, Fachbereich Chemie, Universität Regensburg.

** For the determination of the real and imaginary parts of the dielectric constant, the static conductivity and the phase constant are also necessary, along with the frequency and attenuation constant [1, 2]. The phase constant can be determined using a microwave transmission bridge technique [1, 3, 6]. The conductivity can be measured according to a method developed by Barthel and Walisch [7]. Comprehensive data on low-frequency conductivity, the frequency- and concentration-dependent complex dielectric constants and the dielectric loss angle for all of the substances measured may, upon request, be obtained from the authors.

(25.000 ± 0.0005) °C. The laboratory was thermostatically controlled to (25.0 ± 0.2) °C.

The measurement cell (Fig. 2) is constructed as a concentrical waveguide system which separates the solution-conducting section from the rest of the apparatus by means of two dielectric windows. The scanning probe can be mechanically moved in the x-direction with an accuracy $\Delta x/x \leqq 0.001$. In shifting the probe in the x-direction, a displacement in other directions could not be observed. In the K_A-band cell, the waveguide discontinuity on the left of the cell (Fig. 2) can be avoided by constructing a particularly thin-walled (0.2 mm wall thickness) probe (UG-97/U). By filling the probe with polypropylene ($\varepsilon_r \approx 2.25$) it can be adapted to the frequency-region for the TE_{10}-mode in the UG-96/U-waveguide.

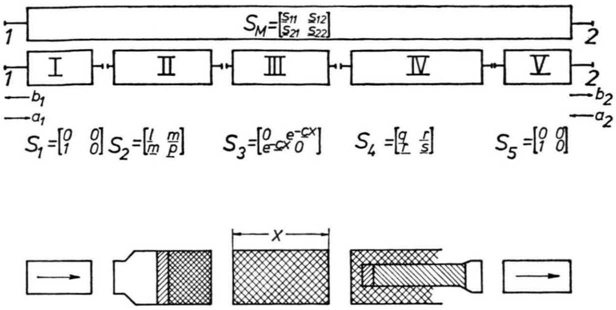

Fig. 2. Schematic representation of the equivalent electrical circuit in terms of 2-port circuits of the measurement instrumentation

$\boldsymbol{l} = l e^{\mathrm{arc}\,\boldsymbol{l}}$, $\boldsymbol{m} = m e^{\mathrm{arc}\,\boldsymbol{m}}$, $\boldsymbol{p} = p e^{\mathrm{arc}\,\boldsymbol{p}}$, $\boldsymbol{c} = \alpha + \mathrm{j}\,\beta$,
x-length of the undisturbed test section in the cell.
$\boldsymbol{q} = q e^{\mathrm{arc}\,\boldsymbol{q}}$, $\boldsymbol{r} = r e^{\mathrm{arc}\,\boldsymbol{r}}$, $\boldsymbol{s} = s e^{\mathrm{arc}\,\boldsymbol{s}}$.

I ideal isolator; II transmissionline window, taper (x-band), basic attenuation; III reflection free path (liquid filled waveguide); IV basic attenuation, probe with window, taper; V ideal isolator.

3. Theory Behind the Determination of the Attenuation Constant

With respect to the theoretical determination of the attenuation constant, it should first be assumed that the behavior of the measurement cell (Fig. 2) can be described by a time independent, linear, sourcefree 2-port (with the scattering matrix S_M). According to its electrical properties, the 2-port S_M would be split into the 2-ports $S_j (j = 1, \ldots, 5)$ (Figure 2). The desired scattering coefficients, $\boldsymbol{s}_{ik} (i, k = 1, 2)$ are obtained by correlating the scattering matrices S_j to their "iterative forms" $C_j (j = 1, \ldots, s)$, multiplying them and calculating back to $\boldsymbol{s}_{ik}$ [1, 4, 13]

$$C_M = \prod_{j=1}^{5} C_j = \begin{bmatrix} c_{M11} & c_{M12} \\ c_{M21} & c_{M22} \end{bmatrix} = \begin{bmatrix} 0 & 0 \\ 0 & \dfrac{1}{\boldsymbol{m} \cdot \boldsymbol{r}} \mathrm{e}^{+\boldsymbol{c}x} - \dfrac{\boldsymbol{p}\,\boldsymbol{q}}{\boldsymbol{m}\,\boldsymbol{r}} \mathrm{e}^{-\boldsymbol{c}x} \end{bmatrix}. \tag{3.1}$$

Therefore, it holds that for $\boldsymbol{s}_{ik}$:

$$\boldsymbol{s}_{21} = \frac{1}{\boldsymbol{c}_{M22}} = \frac{\boldsymbol{m}\,\boldsymbol{r}\,e^{-\boldsymbol{c}x}}{1 - \boldsymbol{p}\,\boldsymbol{q}\,e^{-2\boldsymbol{c}x}},$$

$$\boldsymbol{s}_{22} = \frac{-\boldsymbol{c}_{M21}}{\boldsymbol{c}_{M22}} = 0. \tag{3.2}$$

Since $\boldsymbol{s}_{11} = \boldsymbol{s}_{22} = 0$ holds for the quotient p_1^+/p_2^- of power-flow in port 1 and out of port 2:

$$d(x) = 10 \lg \frac{p_1^+}{p_2^-} \mathrm{dB} = 10 \lg \frac{1}{|\boldsymbol{s}_{21}|^2} \tag{3.3}$$

(d refers to the self attenuation of 2-port S_M).

For $|\boldsymbol{s}_{21}|$ follows:

$$|\boldsymbol{s}_{21}| = \frac{m\,r\,e^{-\alpha x}}{|1 - \boldsymbol{p}\,\boldsymbol{q}\,e^{-2\boldsymbol{c}x}|}. \tag{3.4}$$

As expected, the self-attenuation is a function of x, and, therefore, a function of the length of the liquid column. Only in the case where the minimum distance between the two dielectric windows of the measurement cells (that is, the minimum length of the liquid column) is sufficiently long, then the pass-band damping (basic attenuation) is large enough to minimize the influence of multireflection. When this is the case it follows that the denominator of Eq. (3.4) can be approximated as one, giving the assumed linear behavior of the function $d = d(x)$ [3, 10] which is standard for this experiment. In the experiments, according to this discussion, the above mentioned assumption of linearity was fulfilled in that adjustment to a 30 dB minimum attenuation was always made between the two dielectric windows (Figure 2). In this case, the attenuation curve is a straight line function

$$d(x) = 10 \lg \frac{1}{|\boldsymbol{s}_{21}|^2} = 20 \lg \frac{e^{\alpha x}}{m\,r}. \tag{3.5}$$

Therefore

$$d(x) = \left[\frac{20}{\ln 10}\right] (\alpha\,x - \ln m\,r). \tag{3.5.1}$$

The slope of this straight line is proportional to the attenuation constant α of the solution in question.

Tab. 1. The attenuation constants $\tilde{\alpha}$ and their standard deviations $\sigma(\tilde{\alpha})$ for aqueous electrolytic solutions of different concentrations at 5 frequencies.

KJ	8,2625 GHz		10,015 GHz		11,88 GHz		27,2 GHz		38,5 GHz	
mol/l	$\tilde{\alpha}$	$\sigma(\tilde{\alpha})\cdot 10^{+2}$	$\tilde{\alpha}$	$\sigma(\tilde{\alpha})\cdot 10^{+2}$	$\tilde{\alpha}$	$\sigma(\tilde{\alpha})\cdot 10^{+2}$	$\tilde{\alpha}$	$\sigma(\tilde{\alpha})\cdot 10^{1}$	$\tilde{\alpha}$	$\sigma(\tilde{\alpha})\cdot 10^{1}$
0,5	3,36	0,32	4,25	0,19	5,23	0,42	14,16	0,11	19,75	0,14
1,0	4,28	0,42	5,06	0,28	6,00	0,39	14,55	0,14	20,11	0,19
1,5	5,00	0,36	5,80	0,35	6,59	0,53	14,89	0,12	20,39	0,16
2,0	5,85	0,54	6,60	0,39	7,44	0,39	15,30	0,09	20,71	0,11
3,0	7,12	0,58	7,85	0,67	8,67	0,72	16,01	0,11	21,09	0,20
4,0	8,57	0,81	9,31	0,81	10,19	0,99	16,76	0,15	21,59	0,11
CsF										
0,5	3,26	0,24	4,15	0,18	5,26	0,23	14,19	0,13	19,70	0,12
1,0	3,98	0,22	4,84	0,27	5,93	0,51	14,61	0,15	20,11	0,11
1,5	4,53	0,23	5,39	0,19	6,46	0,48	15,02	0,11	20,25	0,18
2,0	5,16	0,29	6,02	0,46	7,04	0,52	15,36	0,10	20,32	0,15
3,0	5,94	0,43	6,80	0,44	7,81	0,64	15,75	0,14	20,42	0,13
4,0	6,89	0,47	7,76	0,62	8,70	0,65	16,01	0,14	20,38	0,17
KF										
0,5	3,17	0,11	4,11	0,37	5,14	0,37	14,19	0,11	19,61	0,19
1,0	3,86	0,22	4,77	0,39	5,75	0,29	14,40	0,10	19,90	0,11
1,5	4,43	0,34	5,29	0,27	6,27	0,49	14,66	0,09	19,91	0,18
2,0	4,98	0,42	5,81	0,43	6,77	0,52	14,85	0,12	20,02	0,15
3,0	5,84	0,43	6,71	0,49	7,63	0,44	15,16	0,11	19,92	0,11
4,0	6,55	0,61	7,36	0,52	8,44	0,51	15,42	0,15	19,90	0,14
6,0	7,41	0,72	8,16	0,52	9,01	0,79	15,34	0,12	19,36	0,12
8,0	7,70	0,71	8,45	0,78	9,23	0,71	14,71	0,08	17,97	0,16

Results of experiments done on the various electrolyte solutions at fixed frequency were tabulated in tables of the form (d_i, x_i) $(i = 1, 2, \ldots, n, n \geqq 12)$. These data were fitted to straight line attenuation curves (see Eq. 3.5.1) by using the method of least squares. The slopes a, respectively $\tilde{\alpha}$ *, of the straight lines $(a = 20\,\alpha/\ln 10)$ where determined using point estimates. The corresponding standard deviation was also calculated [c. f. Table 1].

The deviation of the observation from the straight line w_i was further analysed according to Wallis and Moore's phase frequency test [9, 11]. This test examines the deviation of data $w_1, w_2, \ldots, w_n$ with respect to randomness. If the sample indicates randomness, then the signs of the differences $(w_{i+1} - w_i)$ should give a random plot (null hypothesis). The alternative hypothesis was, then: The progression of plus and minus signs deviates significantly from randomness. A succession of the same sign will be considered here as a phase, the test being based upon the frequency of plus and minus signs. If the sum of phases is designated by h, with the first and last phase being discarded then, according to the assumption of randomness of a data series,

$$Z = \left\{\left|h - \frac{2n-7}{3}\right| - 0{,}5\right\} \Big/ + \sqrt{\frac{16n-29}{90}} \tag{3.6}$$

is normally distributed and can, with a given statistical certainty (e.g. $p = 0{,}05$), be compared with the limits of the standard normal distribution with a mean value of zero and a standard deviation of one, $N(0, 1)$ (in this case $Z_{\text{krit}} = 1.96$)**. If Z exceeds this value, the existing data series should not be interpreted as random [11]. Too many phases point to a regular "growth", too few to lumpy distribution.

4. Results and Discussion

Table 1 lists the results on aqueous KF-, CsF- and KI-solutions. The percent error in the attenuation constant is consistantly less than or equal to 0.1%. This indicates, specifically for the frequency region between 26.5 and 40.0 GHz, a high degree of accuracy. This accuracy is, however, limited in some cases by the behavior of the random-value Z. In those few data series where the value of Z exceeds

---

* The squiggle over a symbol denotes an estimated value.

** In the consideration of the random test results it is here referred to the region $\mu \pm 1.96$ or $Z = \pm 1.96$ with 95% total amplitude; i.e. the probability p that the absolute value of the result of x minus μ differs by more than $1.96\,\sigma$ (σ standard deviation), is 0.05 $[p(|x-\mu| \rangle 1.96) = 0.05]$.

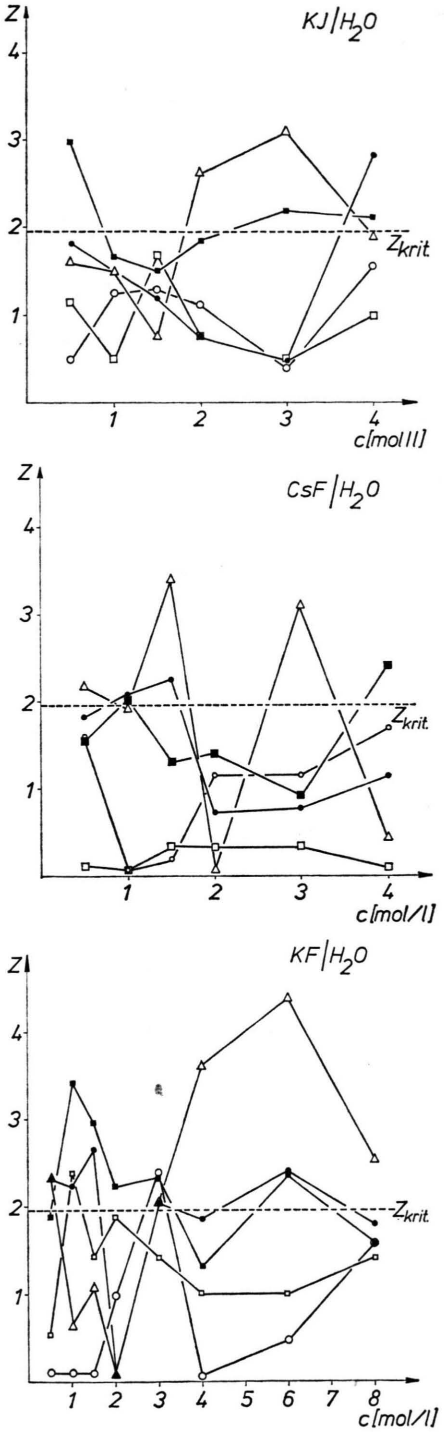

Figs. 3—5. Interpretations of the deviations of the experimental points from the attenuation straight lines plotted in terms of Z-values as a function of concentration for the electrolytes KI-H_2O, CsF-H_2O and KF-H_2O def. according to Gl. 3.6). ● 8,2625; ■ 10,015; △ 11,88; □ 27,2; ○ 38,5 GHz.

that of the critical value Z_{krit}, straight lines are no longer the best fitting curves. In Figures 3 – 5 the Z values are plotted for the different frequencies as a function of the concentration. It can be seen that in the X-band the value of Z frequently exceeds Z_{krit}. In the K_A-band Z exceeds Z_{krit} only twice (KF-H_2O: 1 m at 27.2 GHz and 3 m at 38.5 GHz). In all cases where $Z > Z_{\text{krit}}$, it occurs where the phase frequencies are too low. This results in lumping which can be attributed to the influence of higher order modes[1]. In section 2, the measurement cell was described as a 2-port circuit. This description is not initially applicable in all cases because of the propagation of higher order modes of at least up to TE_{12}-modes. This is a consequence of electrical and mechanical discontinuities at the right end of the measurement cells (Figure 2). These discontinuities create a multiport-junction. One port of this junction is the lower entrance of the measurement probe (rectangular waveguide) and the other is the entrance of the "coaxial cable" formed by the outer conductor of the measurement cell and the probe (coaxial cable with rectangular cross-section). This "coaxial cable" was constructed lengthwise such that when it is filled with solution, it acts as if it were sealed off with an ideal absorber. The transmission line junction is, of course, not reflection free. This establishes the assumptions for the excitation and mixing of higher order modes (waveguide discontinuities, metallic face of the probe, dielectric windows attached in or on the probe face and the polyethylene filling of the tapered probe).

Higher order modes can also be excited in the region of the left dielectric window of the measurement cell (Figure 2). These waves are, depending upon the dielectric in the cell, either propagated or existent as attenuated modes. Initially the air-filled waveguide connected to the measurement probe acts as a filter for all modes higher than the TE_{10}-mode. The influence on the linearity of the function of Eq. (3.5.1) can thereby only come about through a mode mixing which, in this case, occurs by means of a partial transformation of higher order modes in the TE_{10}-mode at the discontinuity in the measurement cell. In the region of the left dielectric window propagatable higher order modes are excited, which are propagated together with the TE_{10}-mode in the cell and which are partially transformed into the TE_{10}-mode in the region of the probe window. The influence of multiple reflections was excluded from the beginning because of the high dielectric loss angle (more than 60 dB basic attenuation for back- and forreflection).

The decisive influence of discontinuities at the left dielectric window is shown up in the results. The Z-value exceeds the critical Z-value in only 5% of all cases ($Z > Z_{\text{krit}}$) in the K_A-band measurement cell which has, in contrast to the X-band-cell, in the left region a homogeneous cross section. (For the X-band cell 58% of the Z-values exceeded Z_{krit}). This is a consequence of the left electrical discontinuity in the X-band cell and, in the case of the KF-solution, also of the properties of the left window. The window in this extreme case was a pure silicon rubber square plug. In the other measurements, a 0.5 mm mica window was used. Silicon rubber windows are especially conductive to the excitation and mixing of higher order modes because of an unavoidable inclusion of air bubbles [12]. The influence of higher order modes is even stronger when small air bubbles are injected between the cell window and the solution.

On the other hand, with the exception of the last mentioned experiment, the average error in the attenuation constant fell within 0.1%. That is, the influence of higher order modes can only be demonstrated in a statistical analysis of the data. Its accuracy however, comes from that of the precision receiver. Although the construction of the K_A-band cell was better with respect to the excitation of higher order modes than that of the X-band cell, the Z-values it measured were frequently in the neighborhood of Z_{krit}. Therefore, the accuracy of the attenuation constants is no longer a question of receiver accuracy, but rather is limited by the excitation of higher order modes.

We should here like to express our thanks to the Deutsche Forschungsgemeinschaft whose generous help made these experiments possible.

---

[1] J. Krüger, Dissertation, Saarbrücken 1973.

[2] Publication in preparation.

[3] J. Barthel, F. Schmithals, H. Behret, Zeitschr. Phys. Chem. Neue Folge **71**, 115 [1970].

[4] H. Brand, Schaltungslehre linearer Mikrowellennetze, Verlag S. Hirzel, Stuttgart 1970.

[5] H. G. Unger, Elektromagnetische Wellen, Verlag Vieweg, Braunschweig 1967.

[6] T. J. Buchanan, Proc. Instr. Electr. Engr. Part III **99**, 61 [1952].

[7] W. Walisch and J. Barthel, Z. Phys. Chem. N.F. **34**, 38 [1962].

[8] Scientific-Altana Proposal Nr. X 41-1-153 Februar 9 (1971) prepared for the Universität des Saarlandes.

[9] W. A. Wallis and G. M. Moore, J. Amer. Statist. Assoc. **36**, 401 [1971].

[10] R. Pottel, Ber. Bunsenges. physik. Chem. **69**, 363 [1965].

[11] E. Schollmeyer, Dissertation, Kiel 1971.

[12] H. Brand, private communication.

[13] R. E. Collin, Foundations for Microwave Engineering, McGraw Hill, New York 1966.